Models for bearings damage detection in induction motors using stator current monitoring

Martin Blödt, Pierre Granjon, Bertrand Raison, Gilles Rostaing

Models for Bearing Damage Detection in Induction Motors Using Stator Current Monitoring

Martin Blödt[1], Student Member, IEEE, Pierre Granjon[2], Bertrand Raison[3], Member, IEEE, and Gilles Rostaing[4]

[1]Laboratoire d'Electrotechnique de Grenoble / Schneider Electric S.A., France, e-mail: martin.blodt@leei.enseeiht.fr
[2]Laboratoire des Images et des Signaux, Grenoble, France, e-mail: pierre.granjon@lis.inpg.fr
[3,4]Laboratoire d'Electrotechnique de Grenoble, Grenoble, France, e-mail: bertrand.raison@leg.ensieg.inpg.fr[3], gilles.rostaing@leg.ensieg.inpg.fr[4]

***Abstract*—This paper describes new models for the influence of rolling-element bearing faults on induction motor stator current. Bearing problems are one major cause for drive failures. Their detection is possible by vibration monitoring of characteristic bearing frequencies. As it is possible to detect other machine faults by monitoring the stator current, a great interest exists in applying the same method for bearing fault detection. After a presentation of the existing fault model, a new detailed approach is proposed. It is based on two effects of a bearing fault: the introduction of a particular radial rotor movement and load torque variations caused by the bearing fault. The theoretical study results in new expressions for the stator current frequency content. Experimental tests with artificial and realistic bearing damage were conducted by measuring vibration, torque and stator current. The obtained results by spectral analysis of the measured quantities validate the proposed theoretical approach.**

***Index Terms*—Induction motor fault diagnosis, bearing damage, motor current signature analysis, airgap eccentricity, torque variations.**

I. Introduction

Induction motors are nowadays widely used in all types of industry applications due to their simple construction, high reliability and the availability of power converters using efficient control strategies. A permanent condition monitoring of the electrical drive can further increase the productivity, reliability and safety of the entire installation.

Traditionally, motor condition can be supervised by measuring quantities such as noise, vibration and temperature. The implementation of these measuring systems is expensive and proves only to be economical in the case of large motors or critical applications. A solution to this problem can be the use of quantities that are already measured in a drive system e.g. the machine's stator current, often required for command purposes. A general review of monitoring and fault diagnosis techniques can be found in [1],[2].

Bearing faults are the most frequent faults in induction machines (41%) according to an IEEE motor reliability study [3], followed by stator (37%) and rotor faults (10%). R. R. Schoen has proposed a model for bearing fault detection in [4] based on the generation of fault related rotating eccentricities. This fault model has been applied in several works [5],[6].

In the present paper, a more detailed approach will be introduced, taking also into account fault related torque variations. Firstly, a short overview of bearing fault types is given in section II, followed by the characteristic vibration frequencies and the existing fault model developed by R. R. Schoen. In the following sections III and IV, the theoretical background for a new model is developed and new expressions for the frequency content of the stator current in case of bearing faults are obtained. Experimental results with different fault types are given in section V, validating different aspects of the theoretical approach.

II. Existing models for bearing fault detection

A. Bearing Fault Types

This paper considers rolling-element bearings with a geometry shown in Fig. 1. The bearing consists mainly of the outer and inner raceway, the balls and the cage which assures equidistance between the balls. The number of balls is defined as N_b, their diameter as D_b. The pitch diameter or diameter of the cage is designated D_c. The point of contact between a ball and the raceway is characterized by the contact angle β.

The different faults occurring in a rolling-element bearing can be classified according to the affected element:

- outer raceway defect
- inner raceway defect
- ball defect

A fault could be imagined as a small hole, a pit or a missing piece of material on the corresponding element.

The definition of these fault types is somehow "artificial" regarding real bearing damages. Nevertheless, this is the only method of distinguishing the different bearing fault effects on the machine. In a realistic case, a combination of these three effects is more likely to be found.

B. Characteristic Frequencies

With each type of bearing fault, a characteristic frequency f_c can be associated. This frequency is equivalent to the periodicity by which an anomaly appears due to the existence of the fault. Imagining for example a hole on the outer raceway: as the rolling elements move over the defect, they are regularly in contact with the hole which produces an effect on the machine at a given frequency.

The characteristic frequencies are functions of the bearing

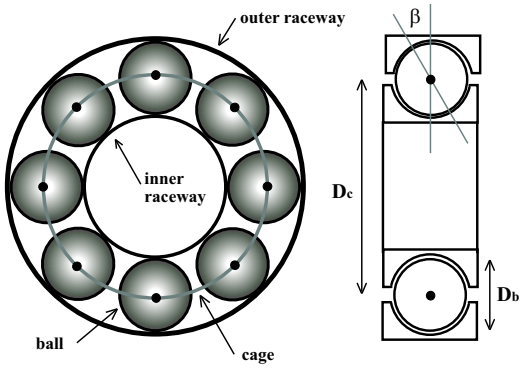

Fig. 1. Geometry of a rolling-element bearing.

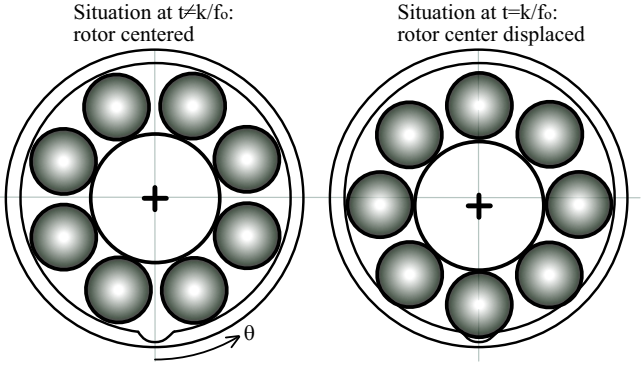

Fig. 2. Radial rotor movement due to an outer bearing raceway defect.

geometry and the mechanical rotor frequency f_r. A detailed calculation of these frequencies can be found in [7]. Their expressions for the three considered fault types are given by:

$$\text{Outer raceway:} \quad f_o = \frac{N_b}{2} f_r \left(1 - \frac{D_b}{D_c} \cos\beta\right) \tag{1}$$

$$\text{Inner raceway:} \quad f_i = \frac{N_b}{2} f_r \left(1 + \frac{D_b}{D_c} \cos\beta\right) \tag{2}$$

$$\text{Ball:} \quad f_b = \frac{D_c}{D_b} f_r \left(1 - \frac{D_b^2}{D_c^2} \cos^2\beta\right) \tag{3}$$

C. Bearing Fault Detection by Stator Current Analysis

The most often quoted model studying the influence of bearing damage on the induction machine's stator current was proposed by R. R. Schoen et al. in [4]. The author considers the generation of rotating eccentricities at bearing fault characteristic frequencies f_c which leads to periodical changes in the machine inductances. This should produce additional frequencies f_{bf} in the stator current given by:

$$f_{\text{bf}} = |f_s \pm k f_c| \tag{4}$$

where f_s is the electrical stator supply frequency and $k = 1, 2, 3, \ldots$.

We consider this model as being incomplete: On the one hand, no detailed theoretical development of the fault related frequency expression is given. On the other hand, it does not consider torque variations as a consequence of the bearing fault. In the following two sections, the existing model will be completed and extended by the means of a detailed theoretical study.

III. Theoretical Study I: Radial Rotor Movement

Two physical effects are considered in the theoretical study when the defect comes into contact with another bearing element:

1. the introduction of a radial movement of the rotor center,
2. the apparition of load torque variations.

The method used to study influence of the rotor displacement on the stator current is based on the MMF (magnetomotive force) and permeance wave approach, traditionally used when considering static and dynamic eccentricity or rotor and stator slotting [8][9] [10].

A. Airgap Length Variations

The first step in the theoretical analysis is the determination of the airgap length g as a function of time t and angular position θ in the stator reference frame. The radial rotor movement causes the airgap length to vary as a function of the defect, which is always considered as a hole or a point of missing material in the corresponding bearing element.

Outer Raceway Defect: Without loss of generality, the outer race defect can be assumed to be located at the angular position $\theta = 0$. When there is no contact between a ball and the defect, the rotor is perfectly centered. In this case, the airgap length g is supposed to take the constant value g_0, neglecting rotor and stator slotting effects. On the contrary, every $t = k/f_o$ (with k integer), the contact between a ball and the defect leads to a small movement of the rotor center in the stator reference frame (see Fig. 2). In this case, the airgap length can be approximated by $g_0(1 - e_o \cos\theta)$, where e_o is the relative degree of eccentricity [11]. In order to model the fault impact on the airgap length as a function of time, a series of Dirac generalized functions can then be used as it is common in vibration analysis [12].

These considerations lead to the following expression for the airgap length:

$$g_o(\theta, t) = g_0 \left[1 - e_o \cos(\theta) \sum_{k=-\infty}^{+\infty} \delta\left(t - \frac{k}{f_o}\right)\right] \tag{5}$$

where e_o is the relative degree of eccentricity introduced by the outer race defect. This equation can be interpreted as a temporary static eccentricity of the rotor, appearing only at $t = k/f_o$.

Inner Raceway Defect: In this case, the situation is slightly different from the outer race defect. The fault occurs at the instants $t = k/f_i$. As the defect is located on the inner race, the angular position of the minimal airgap length moves with respect to the stator reference frame as the rotor turns at the angular frequency ω_r (see Fig. 3). Between two contacts with the defect, the defect itself has moved by an angle described by:

$$\Delta\theta_i = \omega_r \Delta t = \frac{\omega_r}{f_i} \tag{6}$$

Hence, equation (5) becomes:

$$g_i(\theta, t) = g_0 \left[1 - e_i \sum_{k=-\infty}^{+\infty} \cos(\theta + k\Delta\theta_i)\, \delta\left(t - \frac{k}{f_i}\right)\right] \tag{7}$$

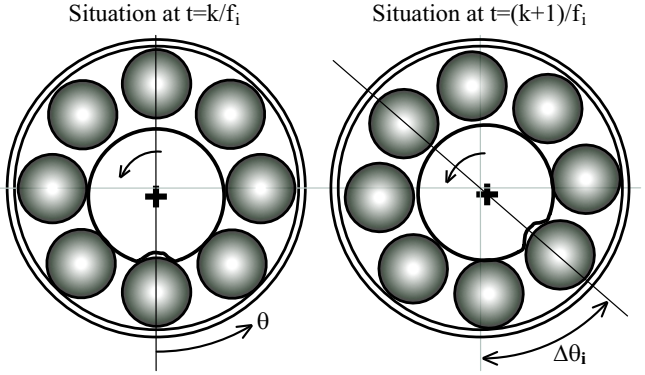

Fig. 3. Radial rotor movement due to an inner bearing raceway defect.

where e_i is the relative degree of eccentricity introduced by the inner race defect.

This equation can be simplified for further calculations by extracting the cosine-term of the sum so that the series of Dirac generalized functions may be later developed into a Fourier series. One fundamental property of the Dirac generalized function is given by the following equation [13]:

$$h\left(k\right)\cdot\delta\left(t-\frac{k}{f_i}\right)=h\left(tf_i\right)\cdot\delta\left(t-\frac{k}{f_i}\right) \tag{8}$$

This formula becomes obvious when one considers that $\delta\left(t-k/f_i\right)$ always equals 0, except for $t=k/f_i$. After combining (8), (7) and (6), the airgap length becomes:

$$g_i\left(\theta,t\right)=g_0\left[1-e_i\cos\left(\theta+\omega_r t\right)\sum_{k=-\infty}^{+\infty}\delta\left(t-\frac{k}{f_i}\right)\right] \tag{9}$$

Ball Defect: In presence of a ball defect, the defect location moves in a similar way as the inner raceway fault. The fault causes an anomaly on the airgap length at the instants $t=k/f_b$. The angular position of minimal airgap length changes in function of the cage rotational frequency. Actually, the balls are all fixed in the cage which rotates at the fundamental cage frequency ω_{cage}, given by [7]:

$$\omega_{cage}=\frac{1}{2}\omega_r\left(1-\frac{D_b}{D_c}\cos\beta\right) \tag{10}$$

The angle $\Delta\theta_b$ by which the fault location has moved between two fault impacts becomes:

$$\Delta\theta_b=\omega_{cage}\Delta t=\frac{\omega_{cage}}{f_b} \tag{11}$$

By analogy with (9), the expression of airgap length in presence of a ball defect becomes:

$$g_b\left(\theta,t\right)=g_0\left[1-e_b\cos\left(\theta+\omega_{cage}t\right)\sum_{k=-\infty}^{+\infty}\delta\left(t-\frac{k}{f_b}\right)\right] \tag{12}$$

where e_b is the relative degree of eccentricity introduced by the ball defect.

Generalization: In order to simplify the following considerations, equations (5), (9) and (12) can be combined in a generalized expression for the airgap length g in presence of a bearing fault:

$$g\left(\theta,t\right)=g_0\left[1-e\cos\left(\theta+\psi\left(t\right)\right)\sum_{k=-\infty}^{+\infty}\delta\left(t-\frac{k}{f_c}\right)\right] \tag{13}$$

where f_c is the characteristic bearing fault frequency given by (1), (2) or (3), and $\psi\left(t\right)$ is defined as follows:

$$\psi\left(t\right)=\begin{cases}0 & \text{for an outer race defect}\\ \omega_r t & \text{for an inner race defect}\\ \omega_{cage}t & \text{for a ball defect}\end{cases} \tag{14}$$

B. Airgap Permeance

The airgap permeance Λ is proportional to the inverse of the airgap length g and is defined as follows:

$$\Lambda=\mu/g \tag{15}$$

where $\mu=\mu_r\mu_0$ is the magnetic permeability of the airgap. In the case of a bearing fault, the permeance becomes with (13):

$$\Lambda(\theta,t)=\Lambda_0\frac{1}{\left[1-e\cos\left(\theta+\psi\left(t\right)\right)\sum\limits_{k=-\infty}^{+\infty}\delta\left(t-\frac{k}{f_c}\right)\right]} \tag{16}$$

where $\Lambda_0=\mu/g_0$.

Firstly, in order to simplify this expression, the fraction $1/(1-x)$ is approximated for small airgap variations by the first order term of its series development:

$$1/(1-x)\approx 1+x \tag{17}$$

The condition $|x|<1$ is always satisfied because the degree of eccentricity verifies $|e|<1$ in order to avoid contact between rotor and stator.

Secondly, the series of Dirac generalized functions is expressed as a complex Fourier series development [13]:

$$\begin{aligned}\sum_{k=-\infty}^{+\infty}\delta\left(t-\frac{k}{f_c}\right)&=f_c\sum_{k=-\infty}^{+\infty}e^{-\mathrm{j}2\pi\mathrm{k}\mathrm{f}_\mathrm{c}\mathrm{t}}\\&=f_c+2f_c\sum_{k=1}^{+\infty}\cos\left(2\pi k f_c t\right)\end{aligned} \tag{18}$$

Equations (16), (17) and (18) can be combined into a simplified expression for the airgap permeance wave:

$$\begin{aligned}\Lambda(\theta,t)\approx\Lambda_0\Big\{&1+ef_c\cos\left(\theta+\psi\left(t\right)\right)\\&+ef_c\sum_{k=1}^{+\infty}\cos\left(\theta+\psi\left(t\right)\pm k\omega_c t\right)\Big\}\end{aligned} \tag{19}$$

where $\cos(a\pm b)$ means $\cos(a+b)+\cos(a-b)$.

C. Airgap Flux Density

The flux density in the airgap is determined by multiplying the MMF (magnetomotive force) with the permeance wave. For the sake of clarity, only the fundamental MMF waves are considered i.e. space and time harmonics are neglected. Rotor and stator fundamental MMFs are waves at supply frequency $\omega_s=2\pi f_s$ with p pole pairs (where p is the pole pair number of the machine). The total MMF F_{tot} is given by their sum and is assumed:

$$F_{tot}(\theta,t)=F\cos(p\theta-\omega_s t+\varphi) \tag{20}$$

Multiplication of (19) and (20) leads to the expression of the flux density distribution $B_{tot}(\theta,t)$:

$$\begin{aligned}B_{tot}\left(\theta,t\right)&=B_0\cos\left(p\theta-\omega_s t+\varphi\right)\\&+B_1\sum_{k=0}^{\infty}\Big[\cos\left((p\pm1)\theta\pm\psi\left(t\right)\pm k\omega_c t-\omega_s t+\varphi\right)\Big]\end{aligned} \tag{21}$$

Equation (21) clearly shows the influence of the rotor displacement caused by the bearing fault on the flux density: In addition to the fundamental sine wave (term B_0), a multitude of fault-related sine waves appear in the airgap. These supplementary waves have $p\pm1$ pole pairs and a frequency content f_{ecc} given by:

$$f_{ecc}=\frac{1}{2\pi}\left(\pm\frac{d\psi\left(t\right)}{dt}\pm k\omega_c-\omega_s\right) \tag{22}$$

In terms of signal processing, these supplementary frequencies result from an *amplitude modulation* of the fundamental sine wave, caused by the modified airgap length.

D. Stator Current

The additional flux density components according to (21) are equivalent to an additional magnetic flux $\Phi(\theta, t)$. By considering the realization of the winding and the geometry of the machine, the additional flux $\Phi(t)$ in each stator phase can be obtained. With stator voltages imposed, the time varying flux causes additional components in the machine's stator current according to the stator voltage equation for the phase m:

$$V_m(t) = R_s I_m(t) + \frac{d\Phi_m(t)}{dt} \tag{23}$$

The frequency content of the flux in each phase is supposed to be equal to the frequency content of the airgap field according to (22). Under the hypothesis of imposed stator voltages, the stator current in each phase is given by the derivative of the corresponding flux. This leads to the following expression for the stator current $I_m(t)$:

$$I_m(t) = \sum_{k=0}^{\infty} I_k \cos\left[\pm \psi(t) \pm k\omega_c t - \omega_s t + \varphi_m \right] \tag{24}$$

It becomes thus obvious, that the radial rotor movement due to the bearing fault results in additional frequencies in the stator current. For the three fault types, these frequencies are obtained from (14) and (24):

Outer race defect: $$f_{\text{ecc or}} = f_s \pm k f_e \tag{25}$$

Inner race defect: $$f_{\text{ecc ir}} = f_s \pm f_r \pm k f_i \tag{26}$$

Ball defect: $$f_{\text{ecc ball}} = f_s \pm f_{cage} \pm k f_b \tag{27}$$

where $k = 1, 2, 3, \ldots$. These expression have not been mentioned in former publications.

In terms of signal processing, it can be noticed that the effect of the fault related rotor movement on the stator current is an amplitude modulation of the fundamental sine wave, due to the effect of the modified permeance on the fundamental MMF wave.

In the previous calculation of the magnetic airgap field, only the fundamental MMF has been considered. Bearing in mind the existence of time harmonics in the MMF, the same additional frequencies will appear not only around the fundamental frequency f_s but also around higher supply frequency harmonics and even around the rotor slot harmonics.

IV. Theoretical Study II: Torque Variations

In this section, the second considered effect of a bearing fault on the machine is studied. Imagining for example a hole in the outer race: each time a ball passes in a hole, a mechanical resistance will appear when the ball tries to leave the hole. The consequence is a small increase of the load torque at each contact between the defect and another bearing element. The bearing fault related torque variations appear at the previously mentioned characteristic vibration frequencies f_c (see section II-B) as they are both of same origin: a contact between the defect and another element.

A. Effect on Rotor MMF

Under a bearing fault, the load torque as a function of time can be described by a constant component Γ_{const} and an additional component varying at the characteristic frequency f_c. This additional component is approximated by a sinusoidally varying function in order to simplify the following considerations:

$$\Gamma_{load}(t) = \Gamma_{const} + \Gamma_c \cos(\omega_c t) \tag{28}$$

where Γ_c is the amplitude of the bearing fault related torque variations and $\omega_c = 2\pi f_c$.

The application of the mechanical equation of the machine leads to the influence of the torque variations on motor speed ω_r:

$$\omega_r(t) = \frac{1}{J} \int_t \left(\Gamma_{motor}(\tau) - \Gamma_{load}(\tau) \right) d\tau \tag{29}$$

where Γ_{motor} is the electromagnetic torque produced by the machine, J is the total inertia of the system machine-load.

In steady state, the motor torque Γ_{motor} is equal to the constant part Γ_{const} of the load torque. This leads to:

$$\begin{aligned} \omega_r(t) &= -\frac{1}{J} \int_{t_0}^{t} \Gamma_c \cos(\omega_c \tau)\, d\tau + C \\ &= -\frac{\Gamma_c}{J\omega_c} \sin(\omega_c t) + \omega_{r0} \end{aligned} \tag{30}$$

The mechanical speed consists therefore of a constant component ω_{r0} and a sinusoidally varying one.

The next step is the calculation of the mechanical rotor angle θ_r which is the integral of the mechanical speed:

$$\theta_r(t) = \int_{t_0}^{t} \omega_r(\tau)\, d\tau = \frac{\Gamma_c}{J\omega_c^2} \cos(\omega_c t) + \omega_{r0} t \tag{31}$$

The integration constant has been supposed equal to zero.

The variations of the mechanical rotor angle θ_r have an influence on the rotor magnetomotive force. In a normal state, the rotor MMF in the rotor reference frame (R) is a wave with p pole pairs and a frequency $s f_s$ and is given by:

$$F_r^{(R)}(\theta', t) = F_r \cos(p\theta' - s\omega_s t) \tag{32}$$

where θ' is the mechanical angle in the rotor reference frame and s the slip.

The transformation between the rotor and stator reference frame is defined by $\theta = \theta' + \theta_r$. Using (31), this leads to:

$$\theta' = \theta - \omega_{r0} t - A_c \cos(\omega_c t) \tag{33}$$

where $A_c = \Gamma_c / (J\omega_c^2)$ is the amplitude of the angle variations.

Thus, the rotor MMF given in (32) can be transformed to the stationary stator reference frame using (33):

$$F_r(\theta, t) = F_r \cos\left(p\theta - \omega_s t - p A_c \cos(\omega_c t) \right) \tag{34}$$

It becomes clear from this expression that the torque variations at frequency f_c lead to a *phase modulation* of the rotor MMF in the stator reference frame. This phase modulation is characterized by the introduction of the term $pA_c \cos(\omega_c t)$ in the phase of the MMF wave.

B. Effect on Flux Density and Stator Current

The airgap flux density B is the product of total MMF and permeance. The airgap length and the resulting permeance are supposed constant in a first time. The *additional* fault related flux density components are obtained by considering the interaction between the modified rotor MMF and the permeance. This leads to:

$$B(\theta, t) = F_{r,1} \Lambda_0 \cos\left(p\theta - \omega_s t - p A_c \cos(\omega_c t) \right) \tag{35}$$

The phase modulation present on the flux density can consecutively also be found on the flux in a machine phase. Considering equation (23), the stator current in phase m is given

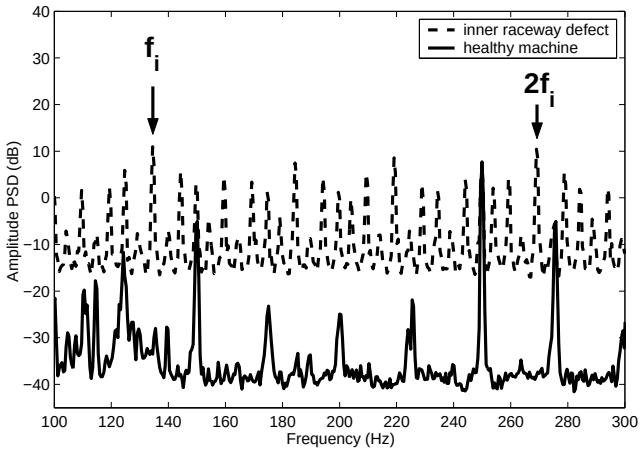

Fig. 4. Vibration spectrum of unloaded machine with inner raceway defect.

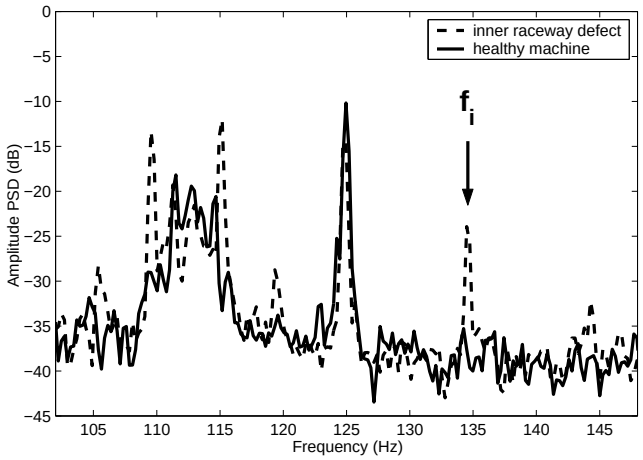

Fig. 5. Torque spectrum of unloaded machine with inner raceway defect.

by the derivation of the flux, leading to the following expression:

$$I_m(t) = I_1 \sin\left(\omega_s t + pA_c \cos\left(\omega_c t\right)\right) \pm I_2 \sin\left(\omega_s t + pA_c \cos\left(\omega_c t\right) \pm \omega_c t\right) \quad (36)$$

The term I_1 conserves the initial phase modulation found on the rotor MMF, the expressions with I_2 result from the derivation and should be of smaller amplitude.

As the frequency content of a sine-wave $x(t) = A\cos\varphi\left(t\right)$ is given by the time derivative of its phase $\varphi\left(t\right)$ (in terms of instantaneous frequency, see [14]), the fault related frequency components in the stator current can be described by:

$$f = \frac{1}{2\pi}\frac{d\varphi(t)}{dt} = f_s - pA_c f_c \sin(\omega_c t) \pm k f_c \quad (37)$$

where $k = 0$ or 1. The effects of the fault related torque variations on the motor current are therefore phase modulations, equivalent to a time varying frequency content.

As in part I of the theoretical study, the time harmonics of rotor MMF and the non-uniform airgap permeance have not been considered. However, the harmonics of supply frequency f_s and the rotor slot harmonics will theoretically show the same phase modulations as the fundamental at f_s.

V. Experimental Results

A. Inner Raceway Defect

A test machine has been equipped with a faulty bearing carrying an inner raceway defect. In a first time, the vibration signal is analyzed. Assuming a contact angle β of zero degrees and motor operating without load ($f_r = 24.96$ Hz), the characteristic inner raceway frequency is calculated from (2) to be 135 Hz.

A logarithmic plot of the vibration spectrum with a damaged bearing in comparison with the healthy machine condition is shown in Fig. 4. The characteristic frequency of the inner raceway defect f_i and its multiples (e.g. $2f_i$) are the components with the largest magnitude. Multiple tests with different load levels permitted to observe slight variations of the characteristic vibration frequency according to equation (2). Additional components due to other mechanical effects and a general rise of the vibration level can also be noticed on the vibration spectrum.

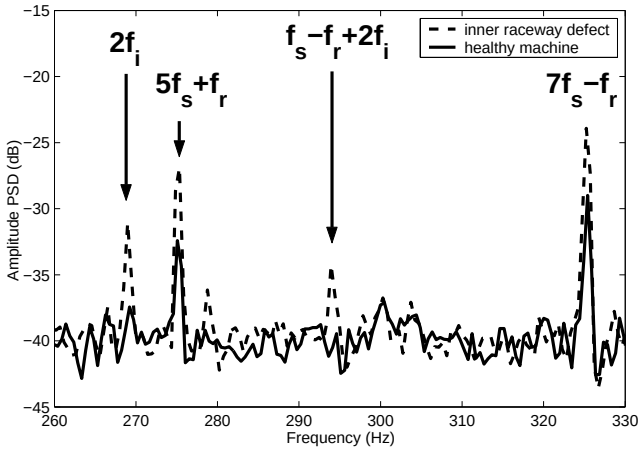

Fig. 6. Stator current spectrum of unloaded machine with inner raceway defect.

A spectral analysis of the measured load torque is shown in Fig. 5. The characteristic fault frequency f_i clearly appears on the torque spectrum with an amplitude of +15 dB in comparison to the healthy case. This validates the proposed theoretical approach which assumes torque variations at the characteristic frequency as a consequence of the bearing fault. Higher harmonics of f_i can also be observed. In addition to the mentioned components, other frequencies appear in the torque spectrum at e.g. 110 and 115 Hz, but they have no direct link to a predicted characteristic frequency.

The stator current spectrum (see Fig. 6) shows, on the one hand, a rise of eccentricity related components at $5f_s + f_r$ and $7f_s - f_r$. These frequency components are already present in the spectrum of the healthy machine due to an inherent level of dynamic eccentricity. The fault related eccentricity increases these components according to (26) (with k=0). The component at $f_s - f_r + 2f_i$ does not appear in the healthy spectrum but in case of the fault as it is consequence of the particular form of eccentricity introduced by the inner raceway fault. Another fault related component at $2f_i$ can be noticed.

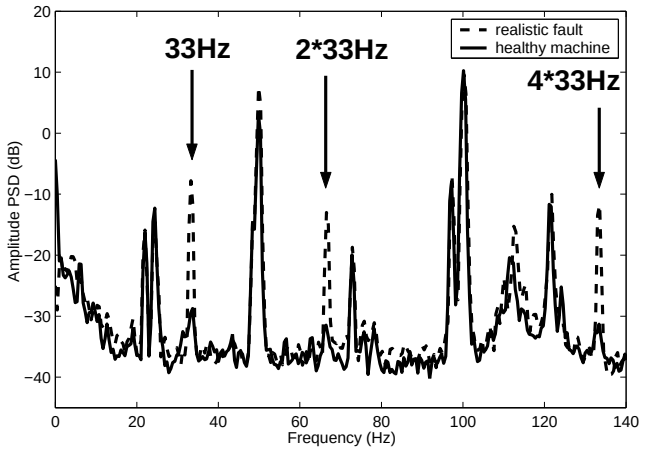

Fig. 7. Torque spectrum of loaded machine with realistic bearing fault.

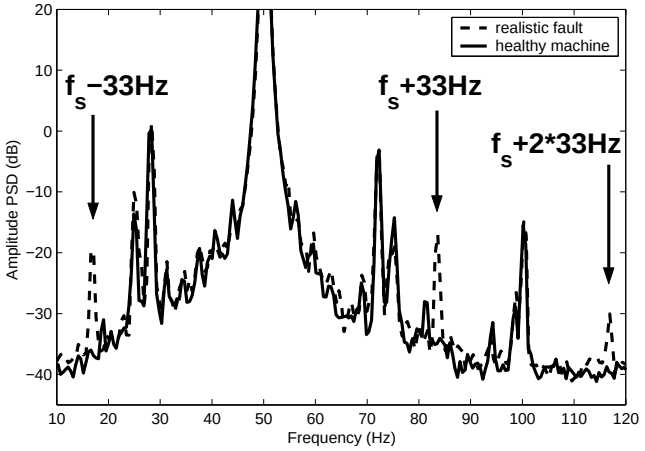

Fig. 8. Stator current spectrum of loaded machine with realistic bearing fault.

B. Realistic Bearing Fault

After the so called ”artificial” bearing faults, tests were conducted with industrially used bearings that have been changed due to a problem, i.e. the fault type is not known.

The tested bearing shows only small effects on the vibration spectrum such as a small peak at 33 Hz. Characteristic vibration frequencies could not be clearly identified. However, the measured machine torque shows considerable changes in comparison to the healthy case (see Fig. 7). At nominal load level, torque variations of great amplitude can be recognized at $k \cdot 33$ Hz.

These torque variations have a considerable effect on the stator current. At Fig. 8, the stator current spectrum with the faulty bearing can be compared to the healthy machine. Sideband components to the fundamental appear at $50 \pm k \cdot 33$ Hz. This is the characteristic signature on the spectrum of a phase modulation of the fundamental [15]. The phase modulation is the consequence of the recognized torque variations as it has been developed in paragraph IV.

VI. Conclusion

This paper has investigated the detection of rolling-element bearing faults in induction motors by stator current monitoring. A new fault model has been proposed which considers fault-related airgap length variations and changes in the load torque. New, more complete expressions for the frequency content of the stator current are obtained for the three major fault types. An experimental study has been conducted on a test rig with several faulty bearings, measuring quantities such as machine vibrations, torque and stator current. The spectral analysis shows that characteristic vibration frequencies are visible in the torque spectrum as it has been supposed in the theoretical study. The torque oscillations lead in consequence to changes in the stator current spectrum. Other fault related components are due to a particular fault-related radial rotor movement.

It has therefore been shown that a detailed analysis of the bearing fault effects leads to fault-related frequency expressions that have not been identified until now. Monitoring these frequencies can improve bearing fault detection.

References

[1] S. Nandi and H. A. Toliyat, “Condition monitoring and fault diagnosis of electrical machines - a review,” in *Proc. IEEE-IAS Annual Meeting Conference ’99*, vol. 1, Phoenix, AZ, Oct. 1999, pp. 197–204.

[2] M. E. H. Benbouzid and G. B. Kliman, “What stator current processing-based technique to use for induction motor rotor faults diagnosis?” *IEEE Trans. Energy Conversion*, vol. 18, no. 2, pp. 238–244, June 2003.

[3] IEEE Motor reliability working group, “Report on large motor reliability survey of industrial and commercial installations,” *IEEE Trans. Ind. Applicat.*, vol. IA-21, no. 4, pp. 853–872, July/Aug. 1985.

[4] R. Schoen, T. Habetler, F. Kamran, and R. Bartheld, “Motor bearing damage detection using stator current monitoring,” *IEEE Trans. Ind. Applicat.*, vol. 31, no. 6, pp. 1274–1279, Nov./Dec. 1995.

[5] B. Yazici and G. B. Kliman, “An adaptive statistical time-frequency method for detection of broken bars and bearing faults in motors using stator current,” *IEEE Trans. Ind. Applicat.*, vol. 35, no. 2, pp. 442–452, Mar./Apr. 1999.

[6] E. L. Bonaldi, L. E. B. da Silva, G. Lambert-Torres, L. E. L. Oliveira, and F. O. Assuncao, “Using rough sets techniques as a fault diagnosis classifier for induction motors,” in *Proc. IEEE IECON’02*, vol. 4, Sevilla, Spain, Nov. 2002, pp. 3383–3388.

[7] B. Li, M. Chow, Y. Tipsuwan, and J. Hung, “Neural-network based motor rolling bearing fault diagnosis,” *IEEE Trans. Ind. Electron.*, vol. 47, no. 5, pp. 1060–1069, Oct. 2000.

[8] J. R. Cameron and W. T. Thomson, “Vibration and current monitoring for detecting airgap eccentricities in large induction motors,” *IEE Proceedings*, vol. 133, no. 3, pp. 155–163, May 1986.

[9] D. G. Dorrell, W. T. Thomson, and S. Roach, “Analysis of airgap flux, current, and vibration signals as a function of the combination of static and dynamic airgap eccentricity in 3-phase induction motors,” *IEEE Trans. Ind. Applicat.*, vol. 33, no. 1, pp. 24–34, Jan./Feb. 1997.

[10] S. Nandi, S. Ahmed, and H. A. Toliyat, “Detection of rotor slot and other eccentricity related harmonics in a three phase induction motor with different rotor cages,” *IEEE Trans. Energy Conversion*, vol. 16, no. 3, pp. 253–260, Sept. 2001.

[11] H. Guldemir, “Detection of airgap eccentricity using line current spectrum of induction motors,” *Electric Power Systems Research*, vol. 64, no. 2, pp. 109–117, Feb. 2003.

[12] P. D. MacFadden and J. D. Smith, “Model for the vibration produced by a single point defect in a rolling element bearing,” *Journal of Sound and Vibration*, vol. 96, no. 1, pp. 69–82, 1984.

[13] J. Max and J.-L. Lacoume, *Méthodes et techniques du traitement du signal et applications aux mesures physiques, Tome 1*. Paris: Masson, 1996.

[14] B. Boashash, “Estimating and interpreting the instantaneous frequency of a signal - Part 1: Fundamentals,” *Proceedings of the IEEE*, vol. 80, no. 4, pp. 520–538, Apr. 1992.

[15] A. B. Carlson, *Communication systems: An introduction to signals and noise in electrical communication*, 3rd ed. New York: McGraw-Hill, 1986.